$$a_{3,2} = k_{1r} \quad \text{(A21)}$$

$$a_{3,11} = k_{1c} \quad \text{(A22)}$$

$$a_{4,12} = k_{1c} \quad \text{(A23)}$$

$$a_{5,13} = k_{1c} \quad \text{(A24)}$$

$$a_{6,7} = k_{1r} \quad \text{(A25)}$$

$$a_{6,14} = k_{1c} \quad \text{(A26)}$$

$$a_{7,6} = k_{1r} \quad \text{(A27)}$$

$$a_{7,15} = k_{1c} \quad \text{(A28)}$$

$$a_{8,15} = k_{1c} \quad \text{(A29)}$$

$$a_{9,1} = k_{c1} \quad \text{(A30)}$$

$$a_{10,2} = k_{c1} \quad \text{(A31)}$$

$$a_{10,11} = k_{cr} \quad \text{(A32)}$$

$$a_{11,3} = k_{c1} \quad \text{(A33)}$$

$$a_{11,10} = k_{cr} \quad \text{(A34)}$$

$$a_{12,4} = k_{c1} \quad \text{(A35)}$$

$$a_{13,5} = k_{c1} \quad \text{(A36)}$$

$$a_{14,6} = k_{c1} \quad \text{(A37)}$$

$$a_{14,15} = k_{cr} \quad \text{(A38)}$$

$$a_{15,7} = k_{c1} \quad \text{(A39)}$$

$$a_{15,14} = k_{cr} \quad \text{(A40)}$$

$$a_{10,8} = k_{c1} \quad \text{(A41)}$$

Solution of the coupled density matrix equations provides the elements $\rho_i^{c(1)}$, which are summed with concentration weighting to give the absorption.

$$\text{Abs}(\nu) = -\text{Im}(c\sum_{i=8}^{16}\rho_i^c + t\sum_{i=1}^{8}\rho_i^t) \quad \text{(A42)}$$

Rearrangement Mechanisms of $B_{12}H_{12}^{2-}$ and $C_2B_{10}H_{12}$

David J. Wales

Contribution from the University Chemical Laboratories, Lensfield Road, Cambridge CB2 1EW, UK. *Received July 24, 1992*

Abstract: Rearrangement mechanisms for $B_{12}H_{12}^{2-}$ and $C_2B_{10}H_{12}$ are deduced by ab initio calculations at the minimal basis set level. In contrast to most previous discussions, but in accord with orbital symmetry considerations, all the transition states are found to have low symmetry; the three carborane isomers of icosahedral $B_{12}H_{12}^{2-}$ interconvert via a complex series of higher energy minima. The results illustrate how these systems adapt to the lack of low-energy orbital-symmetry-allowed pathways and show that the topology of the potential energy surface changes significantly from the borane to the carborane.

Introduction

Speculations about how borane and carborane clusters rearrange have figured in the literature for several decades. The development of powerful orbital symmetry selection rules by the author and co-workers has recently enabled the relative rearrangement rates of these species to be explained, at least qualitatively.[1-4] Two fundamental cluster rearrangement mechanisms have also been characterized by detailed ab initio calculations including the effects of polarization basis functions and electron correlation.[5] One tantalizing problem, in particular, remains to be properly answered, namely the nature of the high-energy rearrangements of icosahedral $B_{12}H_{12}^{2-}$ and the associated carboranes $C_2B_{10}H_{12}$. The earliest work considered various high-symmetry processes, and this pattern has continued in the recent literature,[6] notwithstanding calculations which showed that the highest symmetry structures may be discounted as possible transition states.[1] Orbital symmetry considerations also suggested that lower symmetry, possibly multistep, processes might be involved,[1-3] given that no low-energy orbital-symmetry-allowed mechanisms are available. In this paper the potential energy surfaces of both $B_{12}H_{12}^{2-}$ and $C_2B_{10}H_{12}$ are investigated by ab initio calculations at the minimum basis set level, and numerous reaction pathways are characterized. Hence, this work also provides a detailed investigation of how an inorganic cluster may circumvent the lack of any low-energy orbital-symmetry-allowed pathways. Two key points emerge: (1) The topology of the $C_2B_{10}H_{12}$ potential energy surface is significantly different from that of $B_{12}H_{12}^{2-}$, although there are obvious interrelations. (2) The three carborane isomers of icosahedral $B_{12}H_{12}^{2-}$ probably rearrange via a series of higher energy minima that are linked by generally low symmetry transition states. There are, however, some important caveats that must be established. First, the present results have been obtained from the SCF approximation with a minimal STO-3G basis. Second, the large number of higher energy minima and transition states obtained means that the investigation is incomplete and that the interconversion routes obtained may not be the lowest available. Third, some of the energy barriers involved are rather large, and it is conceivable that excited electronic states could also be involved.

The minimal basis set SCF approach was unavoidable in this study with current computational resources. Each search step required the calculation of analytic first and second derivatives

(1) Wales, D. J.; Stone, A. J. *Inorg. Chem.* **1987**, *26*, 3845.
(2) Wales, D. J.; Mingos, D. M. P.; Lin, Z. *Inorg. Chem.* **1989**, *28*, 2754.
(3) Wales, D. J.; Mingos, D. M. P. *Polyhedron* **1989**, *15*, 1933.
(4) Mingos, D. M. P.; Wales, D. J. *Introduction to Cluster Chemistry*; Prentice-Hall: Englewood Cliffs, 1990.
(5) Wales, D. J.; Bone, R. G. A. *J. Am. Chem. Soc.*, in press.
(6) Gimarc, B. M.; Warren, D. S.; Ott, J. J.; Brown, C. *Inorg. Chem.* **1991**, *30*, 1598.

0002-7863/93/1515-1557$04.00/0

of the energy, with no symmetry constraints. In future work it should, however, be possible to perform more accurate calculations for the higher energy stationary points located in this study, particularly those which possess a mirror plane or axis of rotational symmetry. Recent calculations of the rearrangement mechanisms for $B_8H_8^{2-}$ and $C_5H_5^+$ including polarization basis functions and approximations to the correlation energy provide some measure of encouragement;[5] the topology of the surfaces calculated with minimal basis sets agreed with the highest level calculations, although the energy barriers changed significantly.

There are, of course, many other ab initio studies of boranes and carboranes in the literature. These range from qualitative investigations using simple empirical potentials[7] to studies of the effects of polarization functions and correlation energy upon dissociation energies.[8] There has also been an SCF study of 10- and 12-vertex heteroboranes.[9] However, rather few transition state calculations have been performed previously, and these have generally been for relatively simple species.[10] Indeed, it is remarkable that no transition states have ever been calculated before for either $B_{12}H_{12}^{2-}$ or $C_2B_{10}H_{12}$, given that the rearrangements of these species have been the subject of so much experimental effort and theoretical speculation.

Rearrangements of Boranes and Carboranes

In this section we will briefly review the theory which underlies our current understanding of the relative rearrangement rates of borane and carborane clusters. Previous experimental and theoretical results for icosahedral $B_{12}H_{12}^{2-}$ and the associated carboranes, $C_2B_{10}H_{12}$, are then considered. The remaining sections describe the techniques employed in the current work and the results.

Lipscomb's diamond–square–diamond (DSD) process[11] (Figure 1) plays a key role in the rearrangements of deltahedral clusters that have only triangular faces. In this mechanism an edge common to two triangular faces of a cluster skeleton breaks and a new edge is formed perpendicular to it. DSD rearrangements, single and multiple, concerted and stepwise, have been proposed to rationalize the fluxionality of boranes, carboranes, and metalloboranes.[12-13] King[14] was the first to distinguish between inherently rigid clusters (which contain no degenerate edges) and species for which DSD processes are geometrically possible. Edges of a cluster skeleton are termed degenerate if a DSD rearrangement in which they are broken results only in a permutation of equivalent atoms and not in a change in geometry. We denote a general DSD process by $\alpha\beta(\gamma\delta)$, where α and β are the connectivities of the vertices between which the edge is broken and γ and δ are the connectivities of the vertices between which the new edge is made. For a degenerate DSD rearrangement to be geometrically possible we must therefore have $\alpha + \beta = \gamma + \delta + 2$. Conventionally, one does not count the terminal hydrogen atoms when deriving the connectivity. Degenerate single-DSD processes are geometrically possible only for $B_5H_5^{2-}$, $B_8H_8^{2-}$, $B_9H_9^{2-}$, and $B_{11}H_{11}^{2-}$ of the *closo*-boranes. All the other *closo*-boranes (and their associated carboranes) are found experimentally to be nonfluxional. However, neither $B_5H_5^{2-}$ nor $B_9H_9^{2-}$ is fluxional on the NMR time scale. Gimarc and Ott[15-17] subsequently discovered that both these single DSD processes are "forbidden" by orbital symmetry (in the Woodward–Hoffmann sense[18]) and found a symmetry-allowed double DSD mechanism for $B_9H_9^{2-}$.

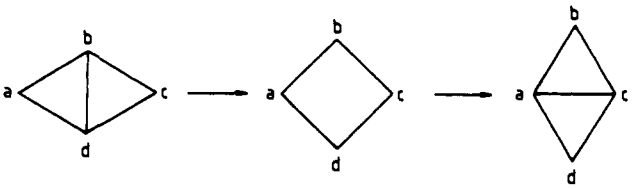

Figure 1. The diamond–square–diamond (DSD) process.

Table I. Stationary Points for $B_{12}H_{12}^{2-}$

point group	energy[40]/h	index	imaginary freq/cm^{-1}
I_h	−299.506 017	0	
C_2	−299.304 910	0	
D_{3h}	−299.275 113	0	
$C_s(A)$	−299.304 266	1	23*i*
$C_s(B)$	−299.286 975	1	93*i*
$C_1(A)$	−299.266 023	1	232*i*
$C_1(B)$	−299.243 462	1	295*i*

Table II. Rearrangement Mechanisms for $B_{12}H_{12}^{2-}$[a]

MIN1	barrier	TS	barrier	MIN2	mechanism
I_h	630.1	$C_1(A)$	23.9	D_{3h}	triangle rotation[b]
I_h	689.3	$C_1(B)$	161.3	C_2	double DSD
C_2	1.7	$C_s(A)$	1.7	C_2	65(54) single DSD single DSD
C_2	47.1	$C_s(B)$	47.1	C_2	stepwise double DSD

[a] MIN1 is the lower energy minimum, TS is the transition state, and MIN2 is the higher energy minimum; the barriers are in kJ mol^{-1}. [b] This unsymmetrical process may also be described as a triple-DSD mechanism.

A general theoretical understanding of the relative rearrangement rates of boranes and carboranes has since been presented within the framework of Stone's tensor surface harmonic (TSH) theory.[4,19] Various orbital symmetry rules may be deduced from this approach; for example, we find that transition states for *closo*-boranes or -carboranes with a single atom on a principal rotation axis of order three or more involve an orbital crossing.[1] In fact, an orbital crossing will generally result for a single-DSD process if a mirror plane is conserved through the critical face.[2] In contrast, if a C_2 axis is retained then there is an avoided crossing and the process is "allowed". Using these rules, and assuming that multiple-DSD processes are less favorable the more DSD components they contain, one may rationalize the relative rearrangement rates of the *closo*-boranes and -carboranes.[1] Similar rules may also apply to transition metal clusters,[2] and second-order Jahn–Teller analysis provides a complementary viewpoint.[3]

More recently, the DSD mechanism has emerged as one of the most important rearrangement mechanisms for various model deltahedral clusters bound by analytic interatomic potentials.[20] Orbital symmetry considerations are not relevant for these molecules and King's topological analysis may sometimes be applied directly to rationalize the relative fluxionalities of these clusters. The results are important in understanding the dynamical behavior of such systems, for example, in developing the theory of solid-like/liquid-like coexistence, as explained elsewhere.[21]

The first obvious statement that can be made about icosahedral $B_{12}H_{12}^{2-}$ and the associated carboranes, $C_2B_{10}H_{12}$, is that there is no geometrically possible degenerate low-order DSD process

(7) Fuller, D. J.; Kepert, D. L. *Inorg. Chem.* **1982**, *21*, 163. Fuller, D. J.; Kepert, D. L. *Polyhedron* **1983**, *2*, 749.
(8) McKee, M. L.; Lipscomb, W. N. *Inorg. Chem.* **1981**, *20*, 4442, 4452. McKee, M. L.; Lipscomb, W. N. *J. Am. Chem. Soc.* **1981**, *103*, 4673. Stanton, R. F.; Bartlett, R. J.; Lipscomb, W. N. *Chem. Phys. Lett.* **1987**, *138*, 525. Stanton, R. F.; Lipscomb, W. N.; Bartlett, R. J. *J. Chem. Phys.* **1988**, *88*, 5726. Stanton, R. F.; Lipscomb, W. N.; Bartlett, R. J.; McKee, M. L. *Inorg. Chem.* **1989**, *28*, 109.
(9) Zahradnik, R.; Balaji, V.; Michl, J. *J. Comput. Chem.* **1991**, *12*, 1147.
(10) McKee, M. L. *J. Am. Chem. Soc.* **1988**, *110*, 5317.
(11) Lipscomb, W. N. *Science* **1966**, *153*, 373.
(12) Wade, K. *Electron Deficient Compounds*; Nelson: London, 1971.
(13) See e.g.: Kennedy, J. D. In *Progress in Inorganic Chemistry*; John Wiley: New York, 1986; Vol. 34.
(14) King, R. B. *Inorg. Chim. Acta* **1981**, *49*, 237.
(15) Gimarc, B. M.; Ott, J. J. *Inorg. Chem.* **1986**, *25*, 83.
(16) Gimarc, B. M.; Ott, J. J. *Inorg. Chem.* **1986**, *25*, 2708.
(17) Gimarc, B. M.; Ott, J. J. *J. Comput. Chem.* **1986**, *7*, 673.
(18) Woodward, R. B.; Hoffmann, R. *Angew. Chem., Int. Ed. Engl.* **1969**, *8*, 781.
(19) Stone, A. J. *Mol. Phys.* **1980**, *41*, 1339. Stone, A. J.; Alderton, M. J. *Inorg. Chem.* **1982**, *21*, 2297. Stone, A. J. *Polyhedron* **1984**, *3*, 1299.
(20) Wales, D. J. *J. Chem. Phys.* **1989**, *91*, 7002. Braier, P. A.; Berry, R. S.; Wales, D. J. *J. Chem. Phys.* **1990**, *93*, 8745. Wales, D. J. *Chem. Phys. Lett.* **1990**, *166*, 419. Wales, D. J. *J. Chem. Soc., Faraday Trans.* **1990**, *86*, 3505. Wales, D. J. *J. Am. Chem. Soc.* **1990**, *112*, 7908. Davis, H. L.; Wales, D. J.; Berry, R. S. *J. Chem. Phys.* **1990**, *92*, 4308. Wales, D. J.; Lee, A. M. *Phys. Rev. A*, in press.
(21) Wales, D. J.; Berry, R. S. *J. Chem. Phys.* **1990**, *92*, 4283.

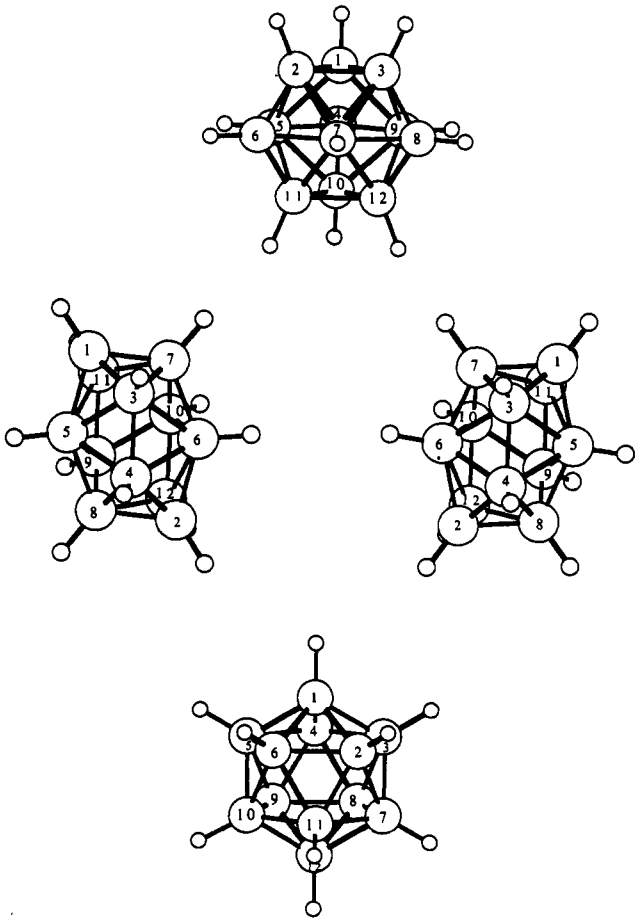

Figure 2. The three minima located for $B_{12}H_{12}^{2-}$. In order of decreasing energy we have D_{3h}, C_2, and I_h geometries. Labeling schemes are indicated in each case, including the two enantiomers of the C_2 structure.

available, and so these species are not "fluxional". However, in 1963 the thermal isomerization of the 1,2 carborane to the 1,7 at around 450 °C was reported.[22] Soon it was also found[23] that the 1,12 isomer can be obtained by heating to around 600 °C. The measured enthalpy activation barrier[24] for the 1,2 to 1,7 interconversion is 260 kJ mol^{-1}, and the barrier for the rearrangement of $B_{12}H_{12}^{2-}$ has been estimated[25] to lie in excess of 335 kJ mol^{-1}. These figures confirm the simplest theoretical conclusion that there are no low-energy rearrangements available for these species. How, then, do the high-energy rearrangements proceed? There are two very appealing symmetrical processes. The first, which may be described as a hextuple concerted DSD process, involves a cuboctahedral transition state;[26] the second, which is describable as a pentuple concerted DSD process (or pentagonal twist), involves a bicapped pentagonal prismatic transition state.[22,27] However, symmetry constrained ab initio calculations for $B_{12}H_{12}^{2-}$ in these O_h and D_{5h} geometries revealed that the former is a saddle point of index 4 while the latter is not a stationary point at all.[1] These results hold for SCF calculations with both STO-3G and 4-31G basis sets. Both structures were also found to lie very high in energy relative to the icosahedral cluster. However, it is interesting to note that both geometries are true transition states for the degenerate rearrangement of a centered 13-atom icosahedron bound by the Lennard-Jones potential[28] (among others).

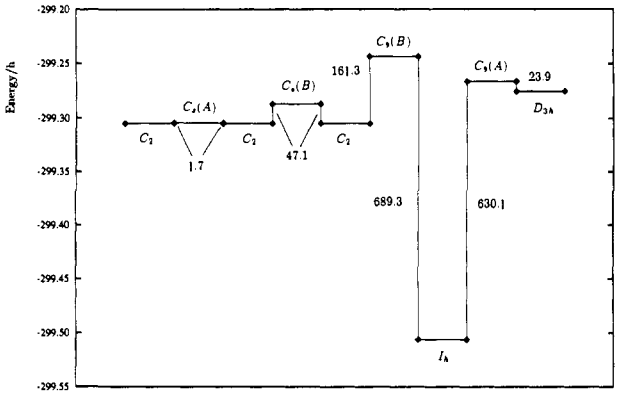

Figure 3. Schematic view of the $B_{12}H_{12}^{2-}$ potential energy surface calculated at the SCF level of theory with a minimal STO-3G basis. The energy scale is in hartrees[40] and the barriers are also indicated in kJ mol^{-1} along with the point groups of the various stationary points (see also Tables I and II).

For the same reasons we can also discount the modified hextuple DSD scheme in which triangular edges of the cuboctahedron are allowed to rotate.[29] The present results further suggest that a *closo-nido-closo* type pathway[30] would probably involve excessive energy barriers. This leaves us with essentially two suggestions outstanding, namely the triangle rotation mechanism first proposed by Zakharkin and Kalinin,[27] and "rediscovered" on several occasions,[1,31] and a series of stepwise DSD processes, as considered elsewhere.[1,2] However, on analyzing the stepwise hextuple and pentuple DSD processes we have previously found that the first and last steps of both schemes would involve orbital crossings for $B_{12}H_{12}^{2-}$, as would the second and penultimate steps of the hextuple DSD process.[1] The present study reveals that three of the four new intermediate structures that occur on these pathways are indeed present as minima or transition states on the $B_{12}H_{12}^{2-}$ and $C_2B_{10}H_{12}$ potential energy surfaces and that all the rearrangements may be characterized as low-order DSD process, both concerted and stepwise.

The lowest energy rearrangement found in this study for $B_{12}H_{12}^{2-}$ entails a barrier of 630 kJ mol^{-1}, and it may be characterized as a distorted triangle rotation mechanism. The introduction of the two carbon atoms introduces greater flexibility, and the largest barrier between the 1,2 and the 1,7 carboranes is calculated to be 311 kJ mol^{-1}; it corresponds to a concerted double-diamond–square–diamond process. In their recent thoughtful experimental contribution,[32] Wu and Jones concluded that a triangle rotation mechanism seemed to be most consistent with their results. Hopefully, the present calculations will help to stimulate further experimental work to isolate some of the new predicted structures and to guide experiments on substituted carboranes.

Method

A modified eigenvector-following[33-35] (EF) algorithm was employed for all the stationary point calculations. In this method searches are conducted which either systematically maximize or minimize the energy with respect to displacements in the directions defined by the eigenvectors of the local second derivative matrix. In a transition state search the energy is maximized in one particular direction (usually the one with the

(22) Grafstein, D.; Dvorak, J. *Inorg. Chem.* **1963**, *2*, 1123.
(23) Papetti, S.; Heying, T. L. *J. Am. Chem. Soc.* **1964**, *86*, 2295.
(24) Salinger, R. M.; Frye, C. L. *Inorg. Chem.* **1965**, *4*, 1815.
(25) Muetterties, E. L.; Knoth, W. H. *Polyhedral Boranes*; Marcel Dekker: New York, 1968; p 69.
(26) Kaczmarczyk, A.; Dobrott, R. D.; Lipscomb, W. N. *Proc. Natl. Acad. Sci. U.S.A.* **1962**, *48*, 729.
(27) Zakharkin, L. I.; Kalinin, V. N. *Dokl. Akad. Nauk SSSR* **1966**, *169*, 590.
(28) Uppenbrink, J.; Wales, D. J. *J. Chem. Soc., Faraday Trans.* **1991**, *87*, 215.
(29) Kaesz, H. D.; Bau, R.; Beall, H. A.; Lipscomb, W. N. *J. Am. Chem. Soc.* **1967**, *86*, 4218.
(30) Wong, H. S.; Lipscomb, W. N. *Inorg. Chem.* **1975**, *14*, 1350.
(31) Reference 25; p 55.
(32) Wu, S.; Jones, M. *J. Am. Chem. Soc.* **1989**, *111*, 5373.
(33) Cerjan, C. J.; Miller, W. H. *J. Chem. Phys.* **1981**, *75*, 2800.
(34) Simmons, J.; Jørgenson, P.; Taylor, H.; Ozment, J. *J. Phys. Chem.* **1983**, *87*, 2745. O'Neal, D.; Taylor, H.; Simmons, J. *J. Phys. Chem.* **1984**, *88*, 1510. Banerjee, A.; Adams, N.; Simmons, J.; Shepard, R. *J. Phys. Chem.* **1985**, *89*, 52.
(35) Baker, J. *J. Comput. Chem.* **1986**, *7*, 385. Baker, J. *J. Comput. Chem.* **1987**, *8*, 563.

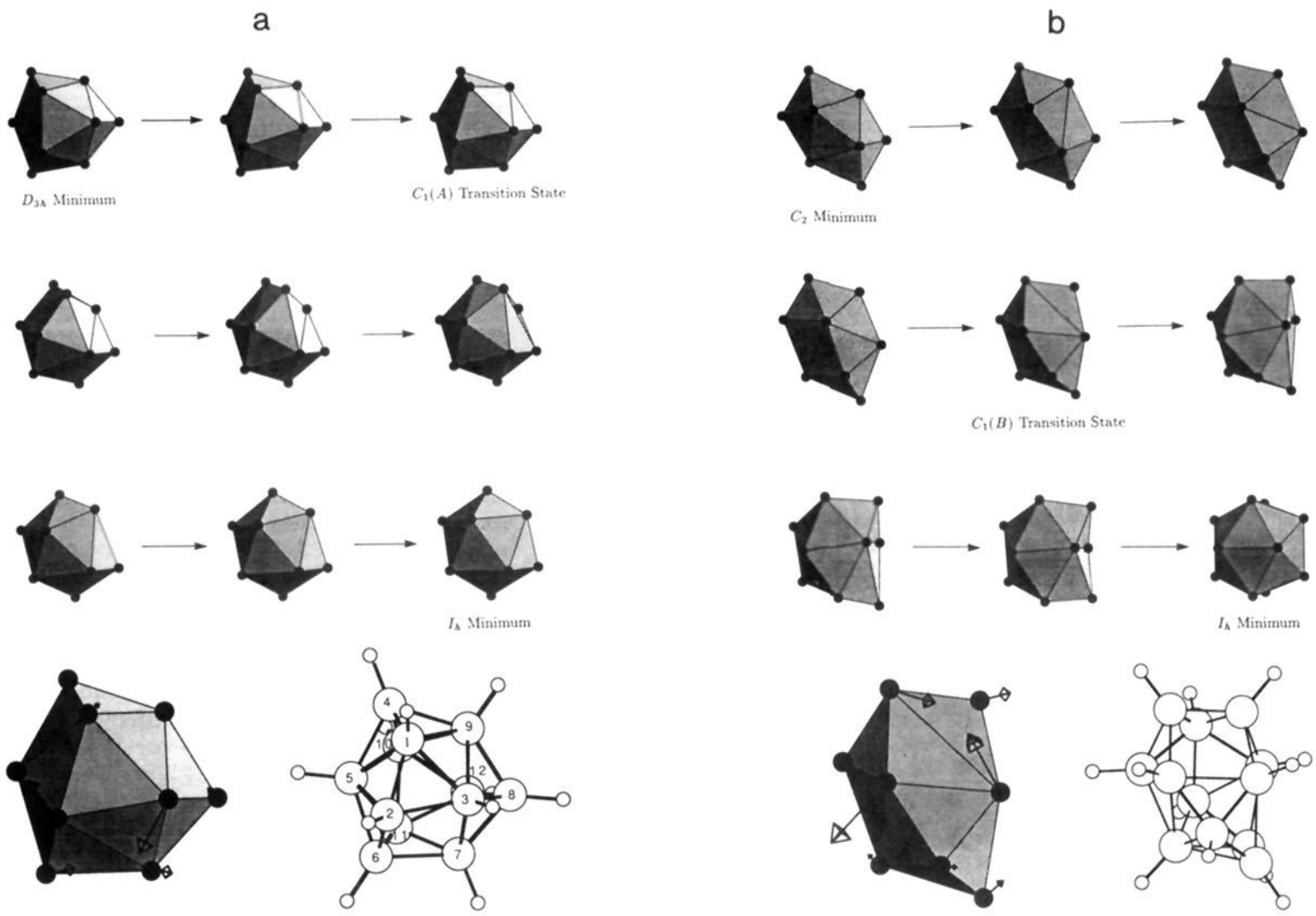

Figure 4. Rearrangement mechanisms for $B_{12}H_{12}^{2-}$. In each case nine geometries along the reaction pathway are illustrated, including the three stationary points. The molecular geometry is represented by triangulating the boron cage and ignoring the terminal hydrogen atoms.[44] Beneath each pathway are two alternative views of the transition state: at the left is an enlargement of the triangulated representation with the normal mode displacements for the forward process added;[44] at the right is a conventional ball and stick plot. (a) D_{3h} to I_h pathway: this may be described as a distorted triangle rotation mechanism, or a triple-DSD process. (b) C_2 to I_h pathway: this may be described as a double-DSD process. (c) Facile rearrangement of the C_2 minimum to produce its enantiomer via a 65(54) single-DSD process. (d) Second, slightly higher energy, rearrangement of the C_2 minimum to its enantiomer via a stepwise double-DSD mechanism. Each step is a 65(54) process.

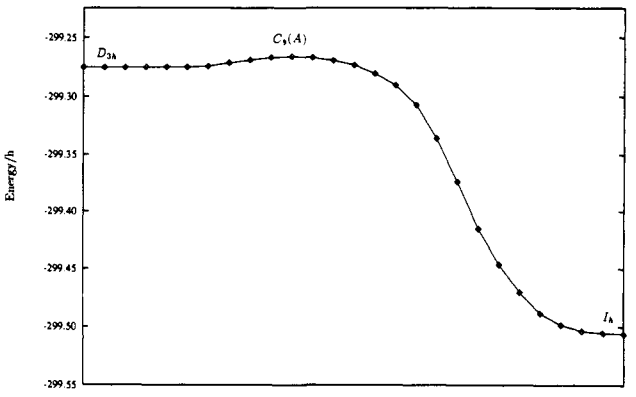

Figure 5. Energy profile for the rearrangement of the $B_{12}H_{12}^{2-}$ D_{3h} minimum to the icosahedron. These are the energies obtained from eigenvector-following searches for minima started from slightly perturbed transition state geometries along the reaction path. The horizontal axis is simply the step number.

Table III. Stationary Points for $C_2B_{10}H_{12}$

point group[a]	energy[40]/h	index	imaginary freq/cm^{-1}
1,12 $I_h \rightarrow D_{5d}$	-325.696 734	0	
1,7 $I_h \rightarrow C_{2v}$	-325.689 465	0	
1,2 $I_h \rightarrow C_{2v}$	-325.654 090	0	
1,2 C_2	-325.579 860	0	
1,3 $C_s(B)$	-325.560 661	0	
1,4 $C_2 \rightarrow C_1$	-325.548 322	0	
1,2 $C_s(C)$	-325.540 423	0	
4,6 $D_{3h} \rightarrow C_s$	-325.535 841	0	
1,8 $C_2 \rightarrow C_1$	-325.532 127	0	
1,4 $C_s(B)$	-325.522 450	0	
2,9 $C_s(B) \rightarrow C_1$	-325.517 092	0	
1,4 $C_s(C) \rightarrow C_1$	-325.508 208	0	
open structure A C_1	-325.492 852	0	
open structure B, C_1	-325.475 846	0	
$C_1(a)$	-325.548 205	1	173*i*
$C_s(b)$	-325.535 656	1	264*i*
$C_1(c)$	-325.535 317	1	207*i*
$C_{2v}(d)$	-325.531 260	1	278*i*
$C_1(e)$	-325.528 481	1	231*i*
$C_1(f)$	-325.515 840	1	337*i*
$C_1(g)$	-325.514 840	1	324*i*
$C_1(h)$	-325.514 840	1	158*i*
$C_1(i)$	-325.501 275	1	267*i*
$C_1(j)$	-325.500 266	1	314*i*
$C_1(k)$	-325.494 070	1	260*i*
$C_1(l)$	-325.492 403	1	295*i*
$C_1(m)$	-325.490 064	1	300*i*
$C_1(n)$	-325.460 638	1	827*i*

[a] The arrow indicates the actual point group when this is different from the parent framework.

Table IV. Rearrangement Mechanisms for $C_2B_{10}H_{12}$[a]

MIN1	barrier	TS	barrier	MIN2	mechanism
1,3 $C_s(B)$	32.7	$C_1(a)$	0.3	1,4 C_2	65(54) single DSD
1,2 I_h	310.9	$C_s(b)$	12.5	1,2 $C_s(C)$	double DSD
1,7 I_h	404.7	$C_1(c)$	1.4	1,4 D_{3h}	triangle rotation[b]
4,6 D_{3h}	12.0	$C_{2v}(d)$	12.0	4,6 D_{3h}	rocking motion
1,2 C_2	134.9	$C_1(e)$	31.4	1,2 $C_s(C)$	triple DSD
1,2 C_2	168.1	$C_1(f)$	42.8	1,8 C_2	double DSD
1,2 C_2	170.7	C_1(g)	20.0	1,4 $C_s(B)$	65(54) single DSD
1,7 I_h	458.5	$C_1(h)$	120.3	1,3 $C_s(B)$	triple DSD
1,7 I_h	494.1	$C_1(i)$	18.2	1,4 $C_s(C)$	double DSD
1,2 C_2	209.0	$C_1(j)$	20.9	1,4 $C_s(C)$	triple DSD
1,8 C_2	99.9	$C_1(k)$	37.1	1,4 $C_s(C)$	triple DSD
1,12 I_h	536.5	$C_1(l)$	78.9	1,4 $C_s(B)$	triple DSD
1,7 I_h	523.5	$C_1(m)$	71.0	2,9 $C_s(B)$	triple DSD
open A C_1	84.6	$C_1(n)$	39.9	open B	terminal H transfer

[a] MIN1 is the lower energy minimum, TS is the transition state, and MIN2 is the higher energy minimum; the barriers are in kJ mol^{-1}. [b] This unsymmetrical mechanism can also be described as a triple-DSD process.

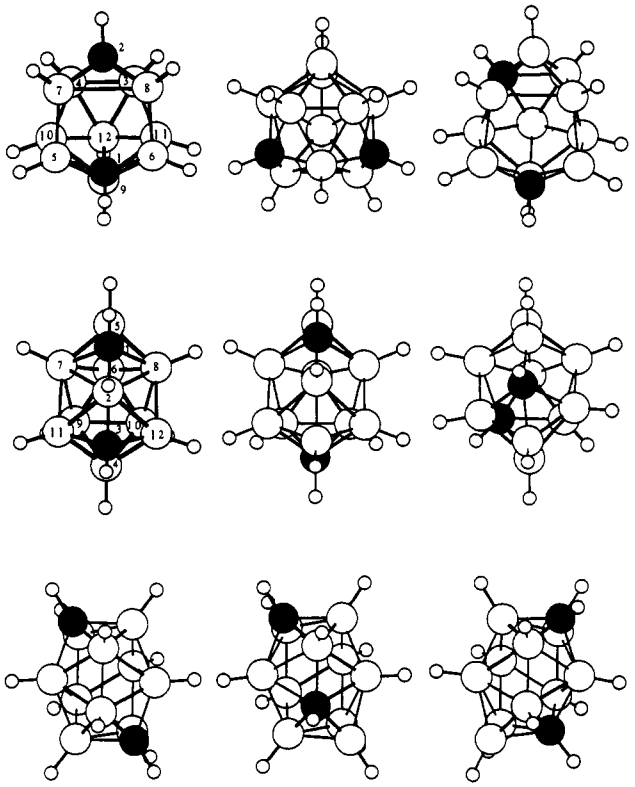

Figure 6. Some of the new minima located for $C_2B_{10}H_{12}$. The energy decreases down the first column, and from right to left within each row. Reading across the rows, starting at the top, we have 1,2 $C_s(C)$, 4,6 D_{3h} (actual point group C_s), 1,4 $C_s(C)$; 1,3 $C_s(B)$, 1,4 $C_s(B)$; 2,9 $C_s(B)$ (actual point group C_1); 1,2 C_2, 1,4 C_2 (actual point group C_1) and 1,8 C_2 (actual point group C_1).

smallest curvature) and simultaneously minimized in all the conjugate directions. Many results have previously been presented for clusters bound by model analytic interparticle forces.[20] These studies have produced further developments in the theory and a better understanding of the behavior of such optimizations.[36,37] A full description of the present method may be found elsewhere;[36,37] the program was originally built upon the ACES package.[38]

The SCF energy and its first and second analytic Cartesian derivatives were calculated using the CADPAC program.[39] $B_{12}H_{12}^{2-}$ and $C_2B_{10}H_{12}$ are, of course, isoelectronic and entail minimal basis sets including 72 functions. Each step required about 85 min of cpu time on a Convex C3840 computer and involved a peak file store usage of about 160 Mb. The cost of performing systematic calculations of this type, with no symmetry constraints, using even a relatively small split-valence basis set such as 4-31G is currently prohibitive. However, constrained optimizations of some of the more symmetrical species found in this study at a higher level of theory should be possible in future work. For each stationary point the magnitude of the maximum component of the Cartesian gradient was reduced to 10^{-6} hartree bohr^{-1} or less,[40] and the six "zero" Hessian eigenvalues were then of order 0.1–1 cm^{-1}. True minima have only real frequencies, corresponding to positive eigenvalues of the mass-weighted second derivative matrix, or Hessian. A true transition state, which is the geometry of highest energy on a minimum energy path between two minima, has precisely one imaginary frequency corresponding to a normal coordinate with negative curvature.[41]

To illustrate the reaction pathways corresponding to each transition state we considered the perturbation of the transition state geometry by adding/subtracting a small fraction of the normal mode corresponding to the unique imaginary frequency. EF searches for minima were then

(36) Wales, D. J. *Mol. Phys.* **1991**, *74*, 1.
(37) Wales, D. J. *J. Chem. Soc., Faraday Trans.* **1992**, *88*, 653.
(38) ACES (Advanced Concepts in Electronic Structure)—An *b initio* Program System: Bartlett, R. J.; Purvis, G. D.; Fitzgerald, G. B.; Harrison, R. J.; Lee, Y. S.; Laidig, W. D.; Cole, S. J.; Trucks, G. W.; Magers, D. H.; Salter, E. A.; Sosa, C.; Rittby, M.; Pal, S.; Stanton, J. F.
(39) Amos, R. D.; Rice, J. E. CADPAC: the Cambridge Analytic Derivatives Package, Issue 4.0; Cambridge, 1987.
(40) 1 hartree = 2.6255 × 10^6 J mol^{-1}, 1 bohr = 0.5291772 × 10^{-11} m.
(41) Murrell, J. N.; Laidler, K. J. *Trans. Faraday Soc.* **1968**, *64*, 317.

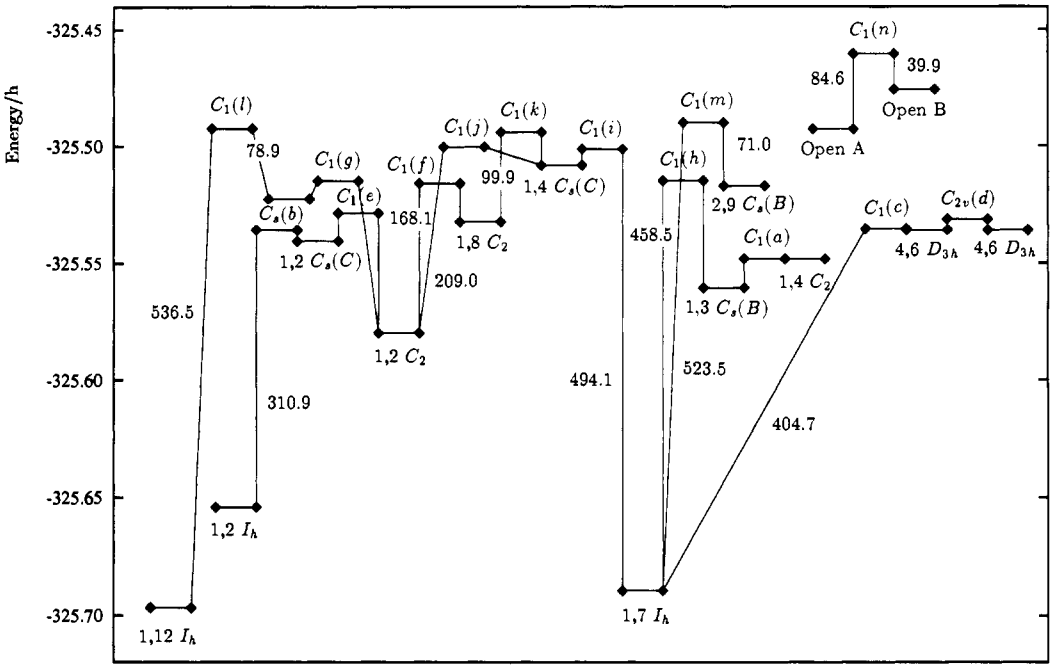

Figure 7. Schematic view of the $C_2B_{10}H_{12}$ potential energy surface calculated at the SCF level of theory with a minimal STO-3G basis. The energy scale is in hartrees[40] and the barriers are also indicated in kJ mol^{-1} (where space permits) along with the point groups of the various stationary points (see also Tables III and IV).

initiated from the two new geometries. This should give us a good representation of the reaction mechanism; the precise relationship between the calculated paths and Fukui's intrinsic reaction coordinate[42] will be discussed elsewhere. They are technically different because the eigenvector-following path is calculated here in internal coordinates, rather than mass-weighted Cartesians. However, the distinction is unlikely to be important, especially since the rearrangements considered involve the motion of B–H (and C–H) units of approximately equal mass.

Results for $B_{12}H_{12}^{2-}$

For $B_{12}H_{12}^{2-}$ three minima and four transition states were located, as summarized in Tables I and II. The minima are shown in Figure 2 with labels for future reference. The energies of the I_h and D_{3h} structures agree with those of Gimarc et al.[6] The latter authors were correct to suspect that the D_{3h} geometry would be the most likely one of the highly symmetrical structures that they considered to mediate a rearrangement process. They were also correct in suggesting that the rearrangement processes in $C_2B_{10}H_{12}$ might be somewhat different, as we shall see in the next section. A schematic view of the potential energy surface is given in Figure 3, and the four rearrangement pathways are illustrated in Figure 4. Two of these mechanisms (corresponding to low barriers and small magnitudes of the transition state imaginary frequency) are rearrangements of the C_2 minimum that produce the enantiomer. A new mirror plane is created (and destroyed) at each transition state, and in accordance with the geometrical symmetry selection rules[43] the transition vector is antisymmetric with respect to these operations. Transition state $C_s(A)$ has a particularly small barrier and was found by following the direction of smallest curvature from the C_2 minimum.

The other two pathways link the two higher energy minima with the icosahedron. For the D_{3h} to I_h pathway the mechanism might be described as an unsymmetrical triangle rotation[27] or as a triple-DSD process. The energy profile for this pathway is shown in Figure 5. The C_2 to I_h mechanism corresponds to a double-DSD process which may be formally written as 55′(55″)/6″5(54′), where the primed and double-primed notation indicates common vertices. Of course, there are two pathways from the two C_2 enantiomers to the icosahedron that are related by a reflection. The C_2 structure and its enantiomer correspond to the middle two geometries encountered on the stepwise pentuple DSD pathway,[1] while the D_{3h} minimum is the central structure in the stepwise hextuple DSD path.[1] These relationships will be further developed in the discussion below.

Results for $C_2B_{10}H_{12}$

Fourteen minima and fourteen transition states were located for $C_2B_{10}H_{12}$, including the three carborane analogues of the $B_{12}H_{12}^{2-}$ icosahedron (Tables III and IV). The energies of the latter structures agree with those reported by Ott and Gimarc.[45] The reader will soon appreciate that an effective nomenclature for these species is of considerable importance, given that there are potentially hundreds of different carborane isomers of the lower symmetry minima. Fortunately, all the minima characterized to date may be identified as substitutional isomers of a small number of basic structures. Four of these were calculated to be stationary points for $B_{12}H_{12}^{2-}$, namely the I_h, D_{3h}, and C_2 minima and the $C_s(B)$ transition state. Apparently the latter species may be sufficiently stabilized by the presence of the two carbon atoms to become a minimum for some substitution patterns. Of course, we would expect the four-connected sites of the cage to be the most favorable places for carbon substitution, as these are the positions where the Mulliken atomic charges are most negative.[46] The other structure, upon which two of the carborane minima are based, is identified as $C_s(C)$ in Tables III and IV. It is related to the D_{3h} geometry by a 65(54) single-DSD process.

EF searches for both a minimum and a transition state were initiated from the 1,4 $C_s(C)$ $C_2B_{10}H_{12}$ geometry, but with boron atoms substituted for the two carbons. These searches led to the icosahedron and the $C_1(B)$ transition state for $B_{12}H_{12}^{2-}$, respectively. Hence the $B_{12}H_{12}^{2-}$ analogue of this structure probably does not exist as a low index stationary point. To identify the carborane minima we therefore refer to the numbering schemes indicated in Figures 2 and 6 for the I_h, D_{3h}, C_2, $C_s(B)$, and $C_s(C)$ structures and write, e.g., 1,4 $C_s(C)$ (which actually has point group C_1). This procedure emphasizes the connections between

(42) Fukui, K. *J. Phys. Chem.* **1970**, *74*, 4162. Fukui, K. *Acc. Chem. Res.* **1981**, *14*, 363.
(43) McIver, J. W.; Stanton, R. E. *J. Am. Chem. Soc.* **1972**, *94*, 8618. Stanton, R. E.; McIver, J. W. *J. Am. Chem. Soc.* **1975**, *97*, 3632.
(44) These plots were produced using Mathematica 2.0, Wolfram Research Inc.
(45) Ott, J. J.; Gimarc, B. M. *J. Comput. Chem.* **1986**, *7*, 673.
(46) Gimarc, B. M.; Ott, J. J. *J. Am. Chem. Soc.* **1986**, *108*, 4298.

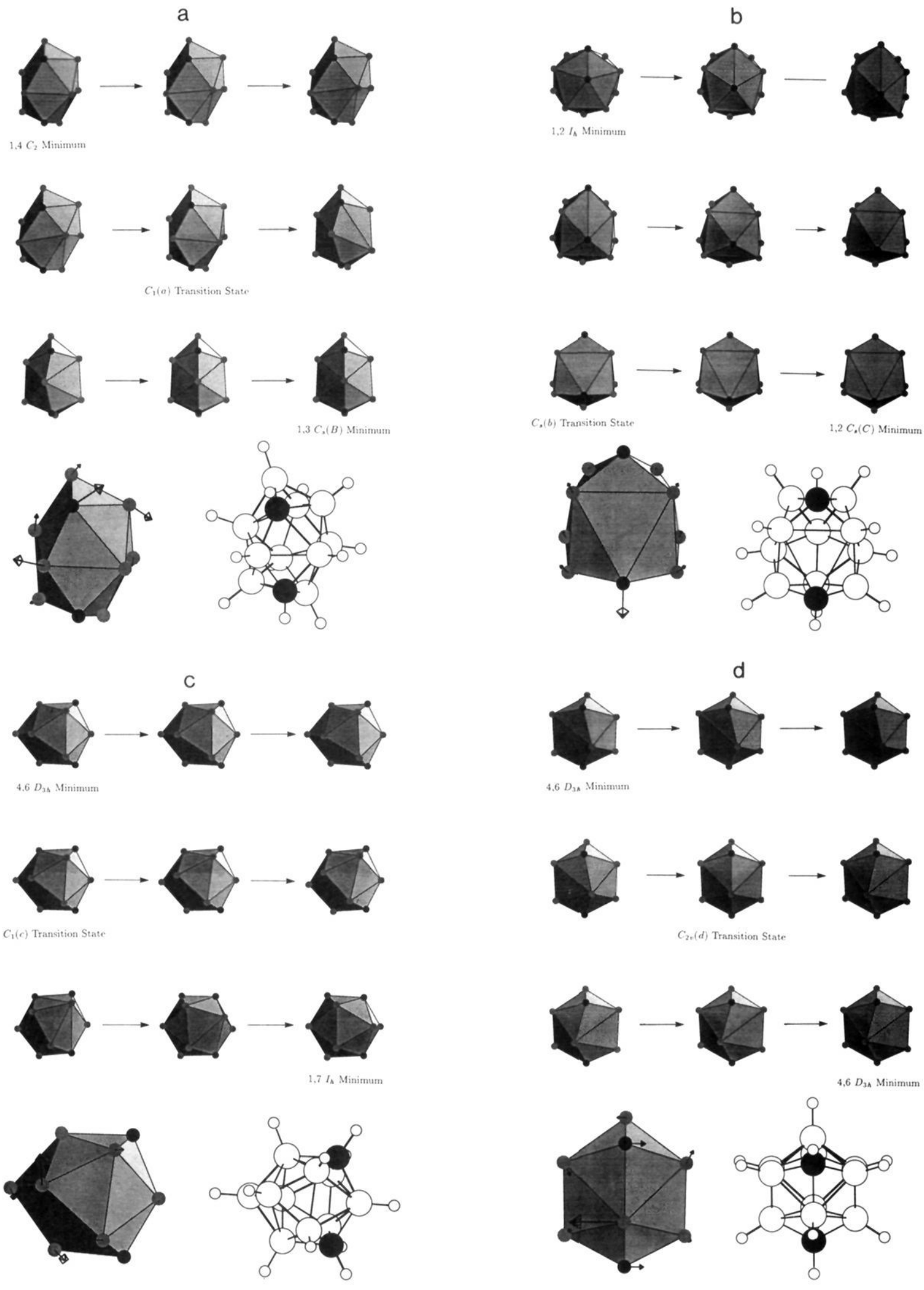

Figure 8. Rearrangement mechanisms for $C_2B_{10}H_{12}$ in the same format as for $B_{12}H_{12}^{2-}$ in Figure 4 arranged in order of increasing energy of the transition state: (a) 1,3 $C_s(B)$ to 1,4 C_2 via $C_1(a)$, 65(54) single-DSD; (b) 1,2 I_h to 1,2 $C_s(C)$ via $C_s(b)$, double-DSD; (c) 1,7 I_h to 4,6 D_{3h} via $C_1(c)$, triple-DSD/triangle rotation; (d) 4,6 D_{3h} to 4,6 D_{3h} via $C_{2v}(d)$, rocking motion; (e) 1,2 C_2 to 1,2 $C_s(C)$ via $C_1(e)$, triple-DSD; (f) 1,2 C_2 to 1,8 C_2 via $C_1(f)$, double-DSD; (g) 1,2 C_2 to 1,4 $C_s(B)$ via $C_1(g)$, 65(54) single-DSD; (h) 1,7 I_h to 1,3 $C_s(B)$ via $C_1(h)$, triple-DSD; (i) 1,7 I_h to 1,4 $C_s(C)$ via $C_1(i)$, double-DSD; (j) 1,2 C_2 to 1,4 $C_s(C)$ via $C_1(j)$, triple-DSD; (k) 1,8 C_2 to 1,4 $C_s(C)$ via $C_1(k)$, triple-DSD; (l) 1,12 I_h to 1,4 $C_s(B)$ via $C_1(l)$, triple-DSD; (m) 1,7 I_h to 2,9 $C_s(B)$ via $C_1(m)$, triple-DSD; (n) open A C_1 to open B via $C_1(n)$, terminal H transfer.

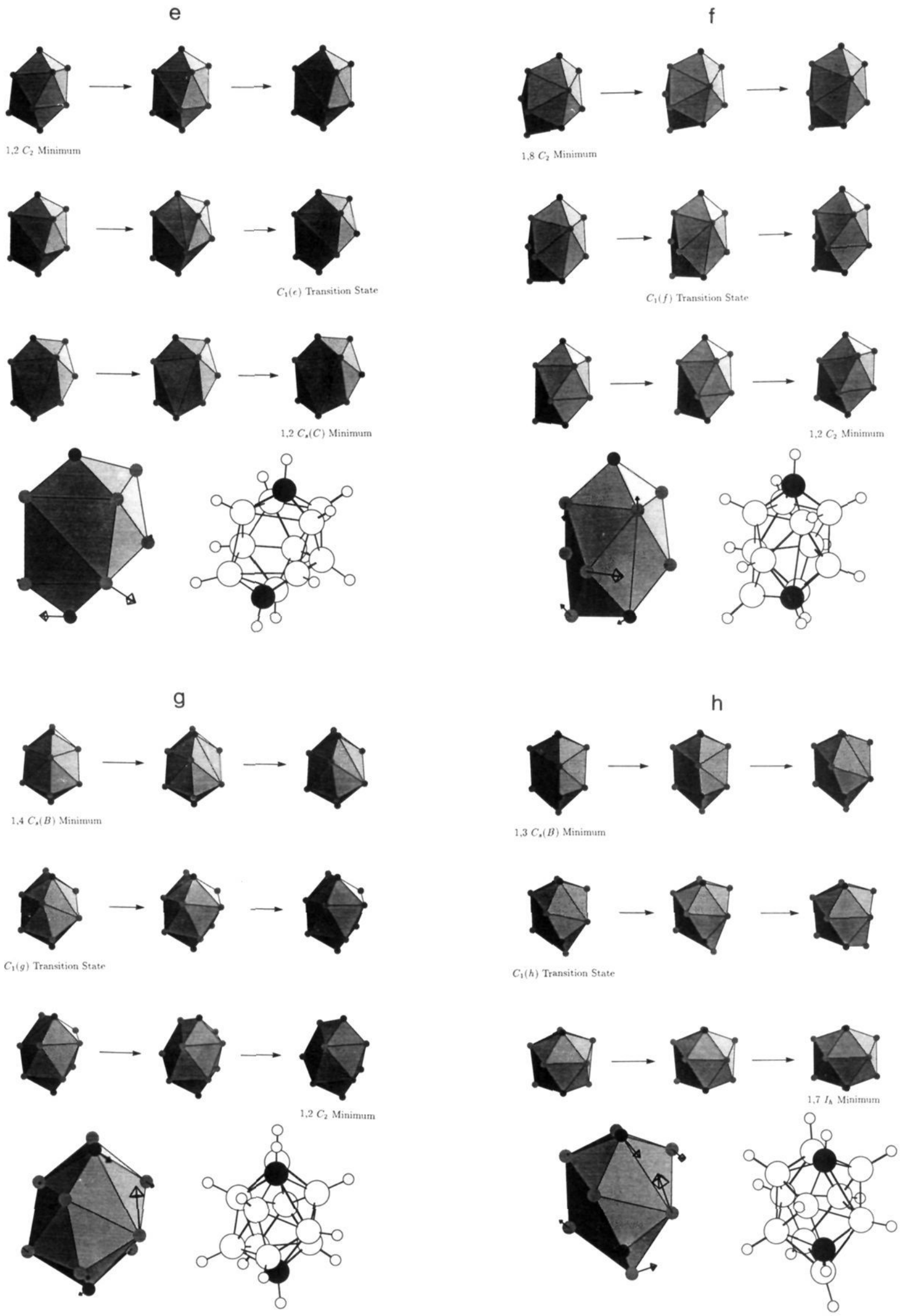

Rearrangement Mechanisms e–h

Figure 8. (continued)

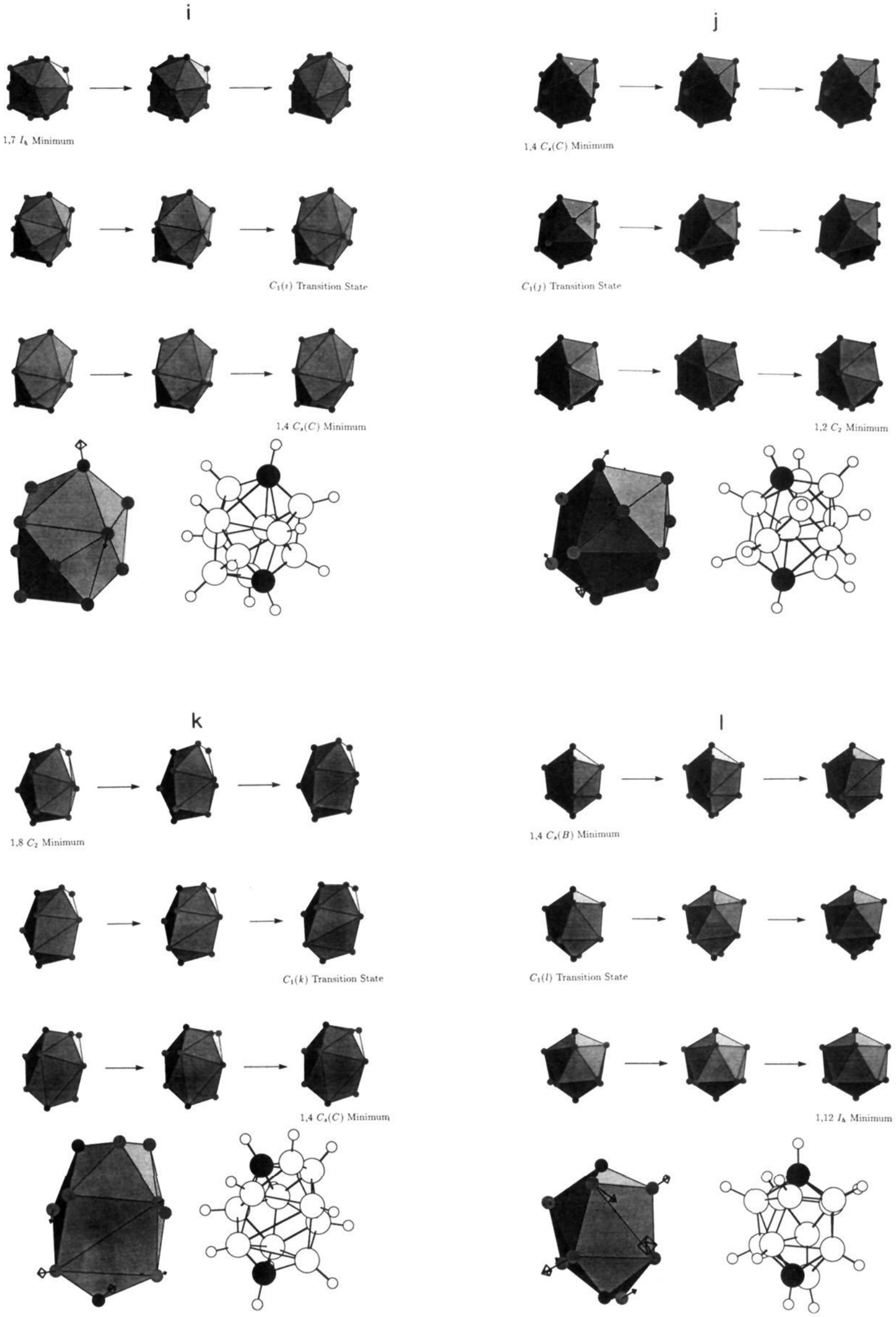

Rearrangement Mechanisms i–l

Figure 8. (continued)

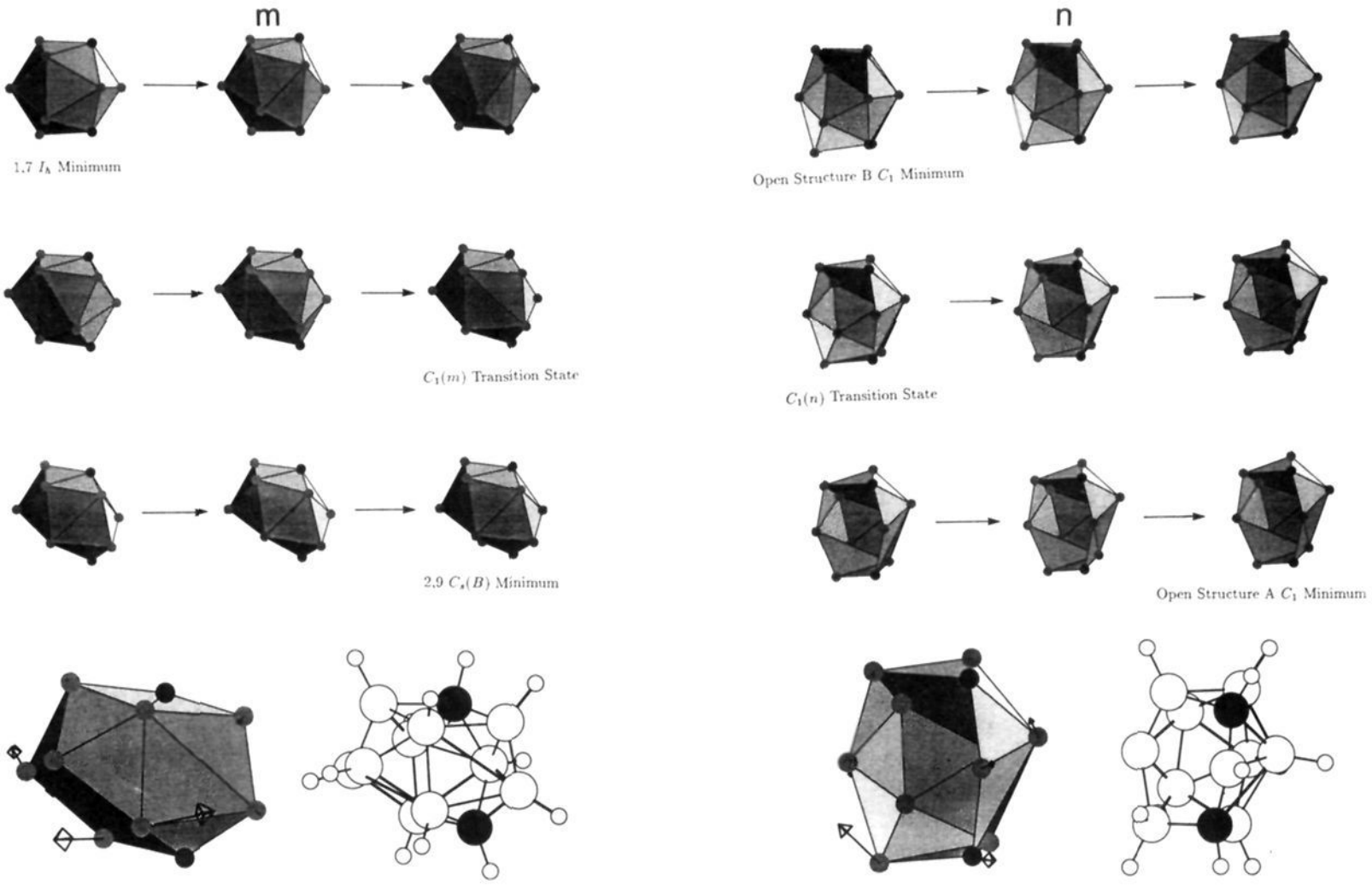

Figure 8. (continued)

the $B_{12}H_{12}^{2-}$ and $C_2B_{10}H_{12}$ results and the structures encountered on the stepwise pentuple- and hextuple-DSD pathways, as discussed in the next section. The transition states simply carry labels a, b, ..., in order of increasing energy, and these correspond to the parts of Figure 8.

Transition states $C_1(a)$ and $C_1(g)$ both link C_2- and $C_s(B)$-type structures via a 65(54) single-DSD process. For $B_{12}H_{12}^{2-}$ the $C_s(B)$ structure is actually a transition state for a rearrangement of C_2 that produces the enantiomer, demonstrating that the carbon substituents perturb the $B_{12}H_{12}^{2-}$ potential energy surface considerably.

Transition states $C_s(b)$ and $C_1(i)$ link I_h- and $C_s(C)$-type structures via a concerted double-DSD process that may be written as 55(5′5)/6′5(55) to indicate that there is one common atom. Although a mirror plane is retained throughout in the mechanism corresponding to $C_s(a)$, the process is orbital symmetry "allowed". Because one edge is broken in the mirror plane and the other is made perpendicular to it, there are two avoided crossings.[2] We note that $C_s(a)$ corresponds to the largest barrier on the path from 1,2 I_h to 1,7 I_h, and the calculated height of about 311 kJ mol^{-1} is reasonably similar to the experimental value[24] for the activation barrier of 260 kJ mol^{-1}. It is also generally true that the incorporation of the heteroatoms reduces the barrier heights, in agreement with Wu and Jones' observations.[32]

Transition state $C_1(c)$ links the 4,6 D_{3h} minimum with the 1,7 I_h carborane and has a very low barrier with respect to the high-energy minimum. This mechanism may be formally described as a triple-DSD process, or as an unsymmetrical triangle rotation (Figure 8c). Transition state $C_{2v}(d)$ mediates a degenerate rearrangement of the 4,6 D_{3h} minimum via a low-energy rocking motion. Again, a new symmetry element is created (and destroyed) at the transition state. Transition state $C_1(e)$ was found by an EF search along the mode corresponding to the smallest Hessian eigenvalue of 1,2 $C_s(C)$ and links the latter structure with a C_2 minimum; $C_1(k)$ corresponds to an analogous rearrangement for a different substitution pattern. This rather complicated process may be formally written as a concerted triple-DSD process 65′(6″4‴)/4′7″(5‴4)/66‴(53″), the first two of which must occur almost synchronously, so that a seven-coordinate vertex is never actually formed. The rearrangement corresponding to transition state $C_1(j)$ also links C_2 and $C_s(C)$ structures, but via a somewhat different pathway (Figure 8j).

Transition state $C_1(f)$ (Figure 8f) represents a double-DSD process (65(55′)/66′(54)) which interconverts C_2 structures; the underlying skeleton undergoes a change of handedness in this process. Neither of the two C_2 to C_2 processes calculated for $B_{12}H_{12}^{2-}$ have yet been identified in $C_2B_{10}H_{12}$. For the $B_{12}H_{12}^{2-}$ $C_s(B)$ transition state this is perhaps not surprising, in view of the fact that several minima have been identified that are based upon this framework. It may well be possible to locate a substituted version of the $B_{12}H_{12}^{2-}$ $C_s(A)$ transition state, but this has yet to be investigated. Transition state $C_1(h)$ was found in EF searches starting from the 2,7-, 3,7-, and 1,9-substituted $B_{12}H_{12}^{2-}$ $C_1(A)$ transition state (labeling scheme in Figure 4a). It links a substituted $C_s(B)$ minimum with a substituted icosahedron, as do $C_1(l)$ and $C_1(m)$. The mechanisms are illustrated in parts h, l, and m of Figure 8 and may each be formally written as a triple-DSD process (as explained below, I_h to C_2 requires two DSD processes, and $C_s(B)$ is obtained from C_2 by a 65(54) single-DSD[47]).

Following a system error (which caused the coordinates to be somewhat scrambled) one transition state search converged to $C_1(n)$, which links two minima with open structures (identified as open structures A and B in Table III). These not only have an open six-membered face, but in each case one of the atoms in the face bears two terminal hydrogen atoms and one bears none at all. In the rearrangement, the extra terminal atom is transferred, and there is a change in the shape of the cluster skeleton. However, these structures are rather high in energy, suggesting that pathways involving open clusters[30] are probably not important.

(47) It is difficult to visualize some of these processes without building models. For this purpose the author strongly recommends the Polydron construction kit, available from toy shops and Eary Learning Centres throughout the UK (and suitable for ages 5 and above!).

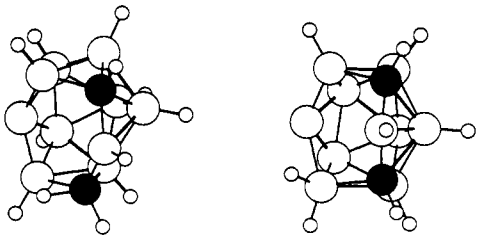

Figure 9. Open structures A (left) and B (right) of $C_2B_{10}H_{12}$.

Discussion

Of course, this study is incomplete in that one would ideally wish to search for transition states and minima from all possible substitution patterns of the D_{3h}, C_2, $C_s(B)$, and $C_s(C)$ structures. There are potentially 66 substitutional isomers for each of $C_s(B)$ and $C_s(C)$, 14 for D_{3h}, and 36 for each C_2 enantiomeric framework. Hence, the surface is even more complicated than that considered[48] by Gimarc et al. for $C_2B_9H_{11}$. The author did indeed consider some of the most potentially interesting substitutions in an attempt to find the lowest energy pathways between the three carborane substituents of icosahedral $B_{12}H_{12}^{2-}$. These were usually, but not always, successful. For example, no analogue of the direct C_2 to I_h pathway has yet been located for $C_2B_{10}H_{12}$; $C_1(j)$ was actually found in a transition state search starting from a substituted version of $B_{12}H_{12}^{2-}$ $C_1(B)$ that would have linked 1,2 C_2 to 1,7 I_h. Additional searches for $B_{12}H_{12}^{2-}$ failed to reveal a transition state between the C_2 and D_{3h} minima.

It is, however, clear how the rearrangements are formally related to the stepwise hextuple- and pentuple-DSD pathways and how the orbital symmetry forbidden steps are circumvented. These connections are illustrated schematically in Figure 10, where the classes of rearrangement and minima found in this study are superimposed upon the formal stepwise paths. Symmetry-allowed double-DSD processes are used to bypass the C_{2v} structures in both schemes. Furthermore, we see that $B_{12}H_{12}^{2-}$ may rearrange via either the C_2 or the D_{3h} structures, while the I_h carboranes are linked directly to the D_{3h}, $C_s(B)$, and $C_s(C)$ geometries. However, the pathways discovered to date involving the D_{3h} structure cannot lead to interconversion of the three I_h carboranes. This would require 2,7-substituted analogues of the $B_{12}H_{12}^{2-}$ D_{3h} minimum and the $C_1(A)$ transition state. A search started from the latter geometry in fact converged to the transition state $C_1(h)$. This is perhaps not surprising, for simple considerations of charge stabilization and electronegativity suggest[46] that the 4,6 D_{3h} geometry should be the most stable. Searching for a minimum from the 1,7-substituted $B_{12}H_{12}^{2-}$ D_{3h} minimum actually led to the 1,2 C_2 carborane.

Conclusions

In conclusion, a number of rearrangement pathways for $B_{12}H_{12}^{2-}$ and $C_2B_{10}H_{12}$ have been calculated within the SCF minimal basis approximation. This has revealed that the vertices of the borohydride may be permuted via two minima of C_2 and D_{3h} symmetry, while the three carboranes based upon an icosahedral framework are interconverted via stepwise processes involving a number of high-energy minima. Some of these minima, particularly the 1,2 C_2 structure, might be viable experimental targets.

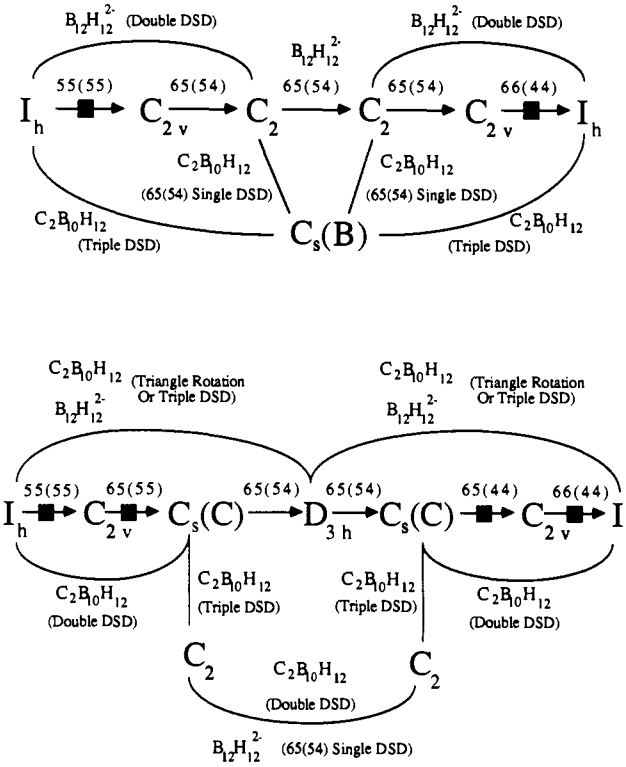

Figure 10. Relation of the structures and rearrangements characterized in the present work to the stepwise pentuple (top) and hextuple (bottom) pathways. The stepwise path is shown horizontally in each case with the observed interconnections drawn around it. The blocks on the stepwise paths indicate rearrangements that are "forbidden" by orbital symmetry in the borohydride. The labels are those used in the present work; only one of the structures on the stepwise path has not been observed in some form, namely the C_{2v} geometry that would arise after a 55(55) single-DSD process from the icosahedron. It may be helpful to note that the 65(54) process is special in that it preserves the total number of 4-, 5-, and 6-connected vertices.

As previously predicted,[1,2] the mechanisms generally involve a small number of concerted diamond–square–diamond (DSD) processes and are related to the stepwise pentuple- and hextuple-DSD pathways. However, where the steps in these pathways are "forbidden" by orbital symmetry, the system effectively steps around them by means of a double-DSD rearrangement. This study has therefore presented the first calculations of true transition states and rearrangement pathways for $B_{12}H_{12}^{2-}$ and $C_2B_{10}H_{12}$ and also provides an illustration of how systems with no low-energy, symmetry-allowed pathways may respond to this restriction. Although more accurate calculations may reveal changes in the precise topology of these surfaces, and lower energy pathways may be found, the principal conclusions of the present work should be unaffected.

Acknowledgment. The author is a Royal Society University Research Fellow. These calculations were made possible thanks to a generous grant of supercomputer time from the SERC.

(48) Gimarc, B. M.; Dai, B.; Warren, D. S.; Ott, J. J. *J. Am. Chem. Soc.* **1990**, *112*, 2597.